

Structural investigation of amorphous iron-nickel-boron alloys

Y. WASEDA, K. T. AUST

Department of Metallurgy and Materials Science, University of Toronto, Toronto, M5S 1A4, Canada

J. L. WALTER

General Electric Corporate Research and Development, Schenectady, New York 12301, USA

Accurate X-ray diffraction investigation has been made of ten amorphous alloys having the compositions $(\text{Fe}_{0.6}\text{Ni}_{0.4})_{100-x}\text{B}_x$ with $x = 14$ to 24 and $(\text{Fe}_{100-y}\text{Ni}_y)_{80}\text{B}_{20}$ with $y = 30$ to 70 which were obtained by rapid quenching from the melt. Using the common Fourier analysis, the radial distribution function was calculated from which the distance and its number of the near neighbour atoms were derived. The present results indicate that the atomic distribution of metallic glasses with low boron content differs slightly from that observed previously for a number of metallic glasses of transition metal-metalloid type. The compositional effect, in particular the boron concentration effect, on the structure and characteristic structural features of amorphous Fe-Ni-B alloy glasses is discussed together with the mean atomic volume and the partial atomic volume of metalloid elements using the measured density data.

1. Introduction

The technique of splat quenching from the liquid state has been extensively used to obtain metallic glasses. The well-known glass-forming metallic alloys are transition metal alloys containing 10 to 30 at % metalloids such as B, C, P and Si. In particular, interest is focused on the various properties of amorphous Fe-B and Fe-Ni-B alloys which have large saturation magnetization and Invar characteristics. Recently the measurements of glass transition and crystallization temperature have been carried out in the amorphous alloy series $(\text{Fe}_{0.6}\text{Ni}_{0.4})_{100-x}\text{B}_x$ and $(\text{Fe}_{100-y}\text{Ni}_y)_{80}\text{B}_{20}$ [1]. The evidence for ordering was the decrease in glass transition and crystallization temperatures with increasing boron in the $(\text{Fe}_{0.6}\text{Ni}_{0.4})_{100-x}\text{B}_x$ series and with increasing nickel in the latter series. This behaviour was opposite to that of the $\text{Fe}_{100-x}\text{B}_x$ series wherein the glass transition and crystallization temperatures increased with increasing boron [1]. Thus, the main purpose of this work is to examine the structure of the Fe-Ni-B alloys with X-ray diffraction and to compare these structures with

those of other amorphous alloys, such as Fe-B and Fe-P systems.

2. Experimental details

The amorphous samples in the series

$$\begin{aligned} & (\text{Fe}_{0.6}\text{Ni}_{0.4})_{100-x}\text{B}_x, \quad x = 14 \text{ to } 24 \\ \text{and} & \\ & (\text{Fe}_{100-y}\text{Ni}_y)_{80}\text{B}_{20}, \quad y = 30 \text{ to } 70 \end{aligned}$$

were prepared in the shape of ribbon (about 0.2 cm wide and 0.003 cm thick) by rapid quenching from the melt. The experimental set-up as well as the procedures for handling the X-ray scattering intensity, the correction of observed intensity data and its analysis, are essentially identical to the procedures employed in the previous works on the structure of metallic glasses [2, 3]. The measurements were carried out in the wave vector (Q) range between 1.0 and 17.0 \AA^{-1} . In the present study, the observed intensity data at Q less than 1.0 \AA^{-1} have been smoothly extrapolated to zero at $Q = 0.0 \text{ \AA}^{-1}$, because the isothermal compressibility data of the Fe-Ni-B glasses are not

available. The effect of this extrapolation and the truncation up to $Q = 17.0 \text{ \AA}^{-1}$ is known to give no critical contribution to the radial distribution function by using the Fourier transformation of Equation 1, as shown in the previous works [4, 5].

$$G(r) = 4\pi r [\rho(r) - \rho_0] = \frac{2}{\pi} \int_0^{\infty} Q i(Q) \sin(Qr) dQ, \quad (1)$$

where $\rho(r)$ is the radial density function, ρ_0 is the average number density of atoms and $i(Q)$ is the so-called reduced interference function directly derived from the measured intensity data.

The density of the samples was measured using the Archimedian method.

3. Results and discussion

We begin with a description of the uncertainty in the structural data obtained in this work. Accumulated intensity counts, varying from 5×10^4 at low angles to 1×10^5 at high angles, were used to hold the counting statistics approximately uniform. The error in the normalization used to evaluate the interference function was determined by Rahman's method [6, 7] and was found to be less than 1.3%. Other sources of systematic error in the X-ray diffraction work of non-crystalline systems were evaluated following the detailed discussion of Greenfield *et al.* [8], leading to an estimate of 2.3% for the total error in the interference function of Fe–Ni–B glasses obtained in this work. Thus, the error bars on $i(Q)$ are of the order of ± 0.06 at the first peak, ± 0.03 near the value $Q = 4.0 \text{ \AA}^{-1}$ and ± 0.02 beyond $Q = 6.0 \text{ \AA}^{-1}$. As a result, the uncertainty in the values of the reduced radial distribution function $G(r)$ is probably similar to that of $i(Q)$, since the computational error was minimized by employing the same procedures [9, 10].

The interference function and the radial distribution function for six samples in the series $(\text{Fe}_{0.6}\text{Ni}_{0.4})_{100-x}\text{B}_x$ are shown in Figs. 1 and 2, respectively. The relevant values such as density and peak positions are listed in Table I. The results for five samples in the series $(\text{Fe}_{100-y}\text{Ni}_y)_{80}\text{B}_{20}$ are given in Figs. 3 and 4 and Table II. The peak positions of $i(Q)$ and $G(r)$ were determined from the position of the apex of the parabola obtained with three points near the peak. The error in these peak positions is of the order of ± 0.01 . The area under each first peak of $4\pi r^2 \rho(r)$ was used to estimate the number of near neighbour atoms,

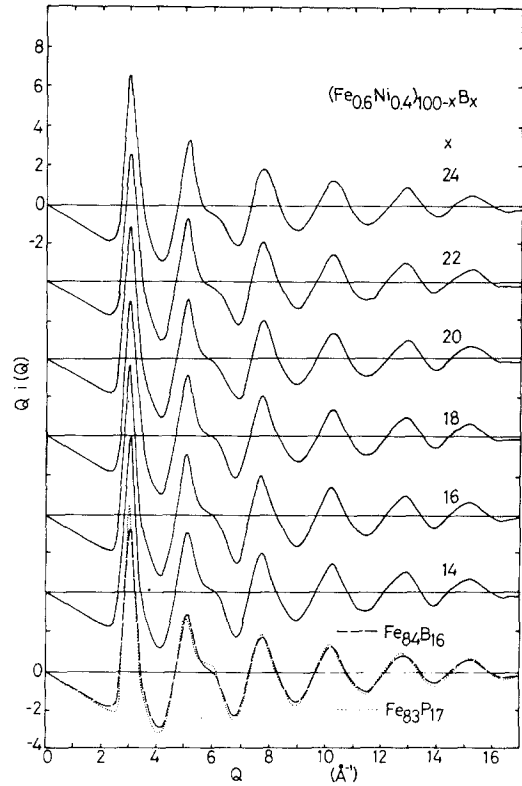


Figure 1 Interference function $i(Q)$ of amorphous $(\text{Fe}_{0.6}\text{Ni}_{0.4})_{100-x}\text{B}_x$ alloys. The results of amorphous $\text{Fe}_{84}\text{B}_{16}$ and $\text{Fe}_{83}\text{P}_{17}$ alloys are taken from the work of Waseda and Chen [3].

n_1 . As we have no unique method of evaluating n_1 [6], only a value obtained by the following equation is given in Tables I and II.

$$n_1 = \int_{r_0}^{r_2} 4\pi r^2 \rho(r) dr, \quad (2)$$

where r_0 is the edge of the left-hand side of the first peak and r_2 corresponds to the first minimum on the right-hand side of the first peak in the $4\pi r^2 \rho(r)$ curves. This method is considered mathematically the best one; however, the validity of this method is doubtful when ripples appear due to the experimental error [6]. Although the present results fortunately are not subject to this problem, the experimental uncertainty in the value of n_1 is difficult to quantitatively estimate. Based on the error in the normalization procedure for evaluating the interference function, an uncertainty of ± 0.5 in n_1 is suggested.

X-ray, neutron and electron diffraction investigation has revealed the general features in the structure of metallic glasses [11]. Thus it is now well accepted that metallic glasses for most of the

TABLE I Density, peak positions and near-neighbour correlation in amorphous $(\text{Fe}_{0.6}\text{Ni}_{0.4})_{100-x}\text{B}_x$ alloys

boron content x	Density (g cm^{-3}) amorphous crystal*		$i(Q)$ (\AA^{-1})			$G(r)$ (\AA)			n_1 (atoms)
			1st	2nd	shoulder	1st	2nd	shoulder	
14	7.82	7.92	3.04	5.25	6.08	2.57	4.29	4.98	11.7
16	7.78	7.94	3.02	5.26	6.07	2.58	4.30	4.98	11.7
18	7.75	7.89	3.02	5.28	6.08	2.58	4.30	4.99	11.9
20	7.70	7.78	2.99	5.26	6.08	2.59	4.32	5.01	12.1
22	7.65	7.72	2.98	5.28	6.10	2.59	4.32	5.01	11.8
24	7.61	7.68	2.98	5.30	6.10	2.58	4.32	5.02	12.3

* After annealing in evacuated quartz capsule at 500°C for 20 min.

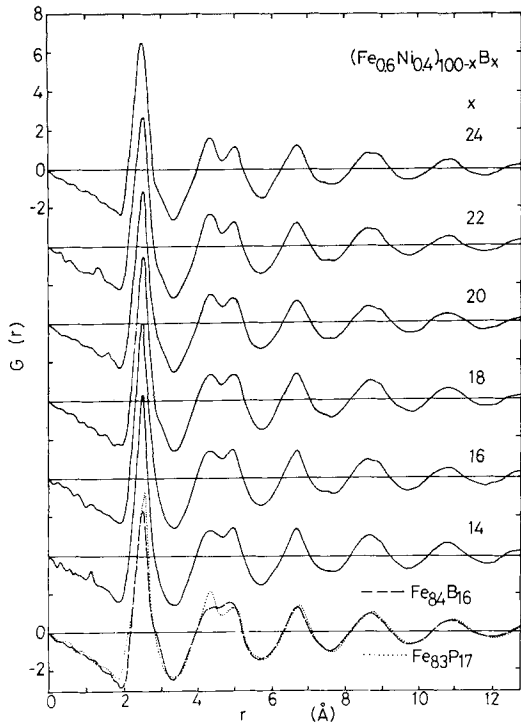


Figure 2 Radial distribution function $G(r)$ of amorphous $(\text{Fe}_{0.6}\text{Ni}_{0.4})_{100-x}\text{B}_x$ alloys. The results of amorphous $\text{Fe}_{84}\text{B}_{16}$ and $\text{Fe}_{83}\text{P}_{17}$ alloys are taken from the work of Waseda and Chen [3].

transition metal-metalloid alloys have the following two characteristic features: (1) a second peak shoulder in the interference function $i(Q)$ is observed; (2) a second peak of the radial distribution function $G(r)$ is split, and the first sub-peak is more intense than the second one.

As shown in the present results of Figs. 1 to 4, the basic profiles of $i(Q)$ and $G(r)$ for amorphous Fe-Ni-B alloys can be classified into the same group as other metallic glasses, i.e. the profile of all samples is composed of a relatively sharp first peak and subsequent smaller oscillations. The second peak shoulder in $i(Q)$ and the second peak

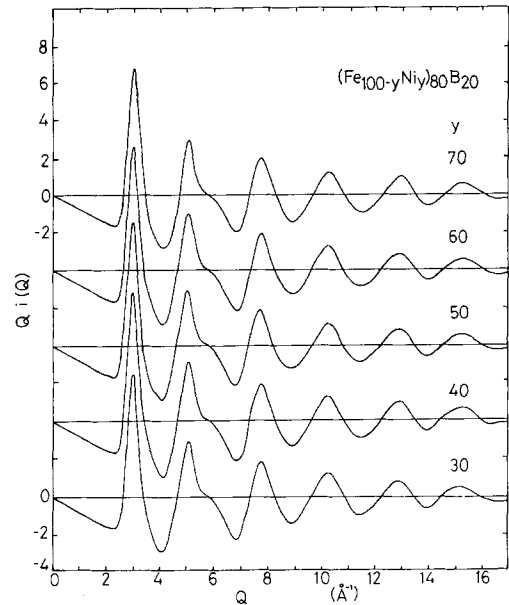


Figure 3 Interference function $i(Q)$ of amorphous $(\text{Fe}_{100-y}\text{Ni}_y)_{80}\text{B}_{20}$ alloys.

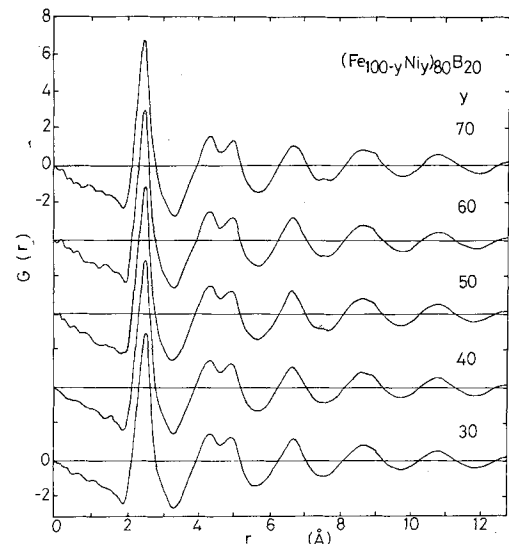


Figure 4 Radial distribution function $G(r)$ of amorphous $(\text{Fe}_{100-y}\text{Ni}_y)_{80}\text{B}_{20}$ alloys.

TABLE II Density, peak positions and near-neighbour correlation in amorphous $(\text{Fe}_{100-y}\text{Ni}_y)_{80}\text{B}_{20}$ alloys

nickel content y	Density (g cm^{-3})		$i(Q)$ (\AA^{-1})			$G(r)$ (\AA)			n_1 (atoms)
	amorphous	crystal*	1st	2nd	shoulder	1st	2nd	shoulder	
30	7.62	7.72	2.98	5.25	6.08	2.59	4.31	5.02	11.9
40	7.70	7.78	2.99	5.26	6.08	2.59	4.32	5.01	12.1
50	7.74	7.87	2.99	5.25	6.06	2.59	4.30	4.98	11.7
60	7.79	7.90	3.00	5.24	6.07	2.58	4.28	4.98	12.2
70	7.84	7.97	3.02	5.24	6.08	2.58	4.28	4.97	12.1

* After annealing in evacuated quartz capsule at 500° C for 20 min.

splitting in $G(r)$ are also observed. Recently, Waseda and Chen [12] reported the anomalous structural behaviour of an amorphous $\text{Fe}_{84}\text{B}_{16}$ alloy, the functions $i(Q)$ and $G(r)$ of which are given in Figs. 1 and 2 for comparison. The anomaly lies in the heights of the sub-peaks of the second peak of the $\text{Fe}_{84}\text{B}_{16}$ (Fig. 2) which are reversed as compared with other amorphous transition metal–metalloid alloys. That is, the height of the right-hand sub-peak (the second sub-peak) of $\text{Fe}_{84}\text{B}_{16}$ is greater than that of the left-hand sub-peak (the first sub-peak) whereas the reverse is true for the Fe–B alloys with 20 at % or more boron and for the more general class of amorphous alloy such as $\text{Fe}_{83}\text{P}_{17}$. For convenience, the function of $G(r)$ for the typical transition metal–metalloid glasses exemplified by amorphous $\text{Fe}_{83}\text{P}_{17}$ is also illustrated in Fig. 2. Similar behaviour in $G(r)$ was also found in the present results with the boron content of 14 and 16 at %, although the first sub-peak of amorphous Fe–Ni–B alloys is more pronounced than that of $\text{Fe}_{84}\text{B}_{16}$, i.e. the sub-peak height ratio of the Fe–Ni–B alloys with 14 and 16 at % boron still differs from that of other transition metal–metalloid glasses. This slight difference in the sub-peak height ratio between $\text{Fe}_{84}\text{B}_{16}$ and $(\text{Fe}_{0.6}\text{Ni}_{0.4})_{84}\text{B}_{16}$ is caused by the compositional effect due to the presence of nickel. With increasing boron content, the first sub-peak is enhanced and the corresponding peak height ratio of the second peak splitting with boron content more than 20 at % becomes similar to that of other transition metal–metalloid glasses. As shown in Figs. 2 and 4, the anomalous structural behaviour in $G(r)$ depends on the boron content but is almost independent of the concentration of metallic elements (Fe and Ni). Since there is no clear difference in the atomic scale structure for the Fe–Ni–B and Fe–B series, the chemical ordering effect between the nickel and boron atoms may play a significant role in the differences

observed by measurements of glass transition and crystallization temperatures [1].

These results imply that the atomic distribution of metallic glasses with boron, particularly with the boron content less than 20 at %, slightly differs from that of other typical transition metal–metalloid glasses. As indicated in the result of an amorphous $\text{Fe}_{84}\text{B}_{16}$ alloy, the anomalous sub-peak height ratio regarding the second peak splitting in $G(r)$ for samples with low boron content is rather close to that of the original calculation of the Dense Random Packing of Hard Spheres (DRPHS) model by Bennett [13]. This contrasts with the extended calculation by the relaxed Bennett model [14, 15] which gives the sub-peak height ratio more like that of $\text{Fe}_{83}\text{P}_{17}$. The different peak profile of metallic glasses with boron content less than 20 at % is of considerable interest and consistent with the experimental results on sputtered film of $\text{Fe}_{78}\text{B}_{19}\text{C}_3$ [16], liquid $\text{Fe}_{83}\text{B}_{17}$ [17] and the model calculation by Boudreax [18, 19], although there is difference in detail. Recently, Yamamoto *et al.* [20] reported a similar peak profile in $G(r)$ of amorphous iron using computer simulation. They also indicated that the frozen-in structure of the liquid state strongly depends on the quenching conditions and the composition and thus the appearance of the different structural characteristics in metallic glasses is quite realistic. In addition, recent experimental results of Fe–B and Fe–Ni–B alloys suggest that hypereutectic alloys consist of a single amorphous phase, whereas hypoeutectic alloys involve two amorphous phases [21]. However, no definite reasons for the anomalous behaviour of metallic glasses with boron could be drawn from the present structural data by X-ray diffraction.

Based on the previous experimental data and model calculations for several kinds of metallic glasses, it may be said that the atomic distribution of metallic glasses with boron depends mainly

upon the dense random packing type structure of transition metal atoms (Fe and Ni) in which the boron atoms, of relatively small size, occupy the vacant space formed by the transition metal elements. This model leads to the relatively high density of the glasses and is consistent with the measured densities for samples investigated which are only 1 to 2% less than the crystalline values (see Tables I and II). Thus, a deformed crystalline-like feature may partly contribute to the short-range order such as the near-neighbour correlations in metallic glasses with boron. Of course, the present authors hold the view that these crystalline-like features are not exactly the same as those in the crystalline state.

As is easily expected from the size factor of transition metal and metalloid elements, the expansion of metal-metal atom distance is unavoidable in the configuration of the above-type structure. This is supported by the results in Fig. 5, i.e. the position of the first peak in $G(r)$ which corresponds to the metal-metal atom distance increases with increasing boron content. The observed expansion is much smaller than that of metallic glasses with phosphorus [11]. This is related to the situation that the diameter of a boron atom is smaller than that of a phosphorus atom. A slight decrease was also observed beyond the boron content of 20 at %.

The above features must be related to the variation of mean atomic volume and the partial atomic volume occupied by metalloid elements

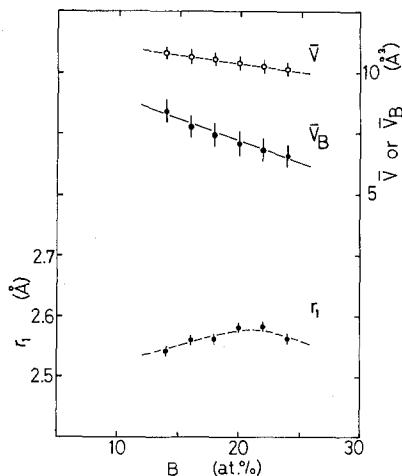


Figure 5 Near-neighbour distance r_1 , mean atomic volume \bar{V} , and partial atomic volume of boron \bar{V}_B , versus boron concentration x for amorphous $(\text{Fe}_{0.6}\text{Ni}_{0.4})_{100-x}\text{B}_x$ alloys.

with metalloid concentration. The mean atomic volume, \bar{V} , is evaluated from measured density data. The partial atomic volume of metalloid elements, \bar{V}_B , could be estimated by the following procedure. According to Turnbull [22], the partial atomic volume of \bar{V}_B is given by:

$$\bar{V}_B = [\bar{V} - (1 - c_B)V_{\text{TM}}^0]/c_B, \quad (3)$$

where c_B is the atomic fraction of metalloids, V_{TM}^0 is the mean atomic volume of the transition metal component in the close-packed crystalline state at room temperature. This assumption for V_{TM}^0 introduces little error, because the volume change on crystallization of metallic glasses is quite small (only 0.4 to 0.5% change) [23]. The value of V_{TM}^0 of amorphous Fe-Ni-B alloys was determined by using the lattice constant of the face centred cubic solid solution of $\text{Fe}_{0.6}\text{Ni}_{0.4}$ [24] and the value of V_{TM}^0 used in this work was 11.11 \AA^3 .

The results of \bar{V} and \bar{V}_B are given in Fig. 5 as a function of boron content. The values of \bar{V} show a linear dependence of the boron concentration. The variation of partial metalloid volume \bar{V}_B is also found to have nearly a linear dependence, but to decrease more rapidly with increasing boron content compared with that of \bar{V} . At the present time, we have no definite information on the size factor of boron in metallic glasses. The covalent radius and the metallic radius of boron are 0.82 and 0.98 \AA , respectively. These values give the effective volume for boron in a close-packed structure of 3.12 and 5.32 \AA^3 . The latter value is close to the effective volume of boron in Fe_2B (5.45 \AA^3) and Ni_3B (5.61 \AA^3) based on the crystalline borides data [25]. From these calculations, we may suggest that the effective volume of boron is 5 to 6 \AA^3 as an example. The present results of Fig. 5 indicate that \bar{V}_B approaches the value of 5 to 6 \AA^3 with higher boron content at 24 at % boron, close to the maximum value for which an amorphous phase can be obtained by rapid quenching from the melt. On the other hand, the value of \bar{V}_B is apparently larger than the value of the effective volume of boron (5 to 6 \AA^3) in the case of lower boron content and thus one may say that the atomic configuration in low boron content glasses involves a relatively large amount of unfilled vacant space by boron and this unfilled vacant space rapidly decreases with increasing boron concentration. These ideas agree well with the picture of transition metal-metalloid glasses first

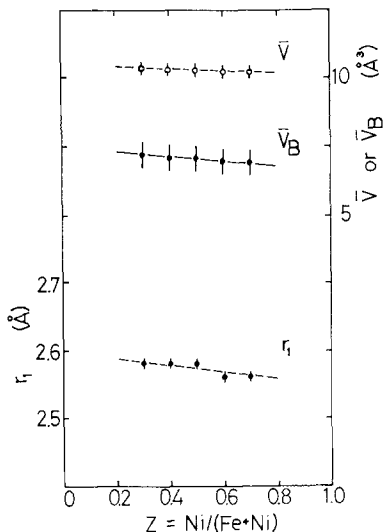


Figure 6 Near-neighbour distance r_1 , mean atomic volume \bar{V} , and partial atomic volume of boron \bar{V}_B , versus nickel concentration z for amorphous $(\text{Fe}_{100-y}\text{Ni}_y)_{80}\text{B}_{20}$ alloys, where $z = \text{Ni}/(\text{Fe} + \text{Ni})$.

proposed by Polk [26]. For a model structure of transition metal-metalloid glasses, Polk suggested that metalloid elements occupy the interstitial holes (so-called Bernal holes) in the DRPHS matrix formed by transition metal elements and the complete occupancy of the holes occurs at about a metalloid content of 20 to 25 at %.

As shown in Fig. 6, the effect of replacing iron by nickel on the structure of amorphous $(\text{Fe}_{100-y}\text{Ni}_y)_{80}\text{B}_{20}$ alloys is insignificant, i.e. the quantities of r_1 , \bar{V} and \bar{V}_B show a linear dependent function of nickel concentration and their change is small compared with the changes as a function of boron concentration given in Fig. 5. This is evident from the fact that the size factor difference between an Fe and an Ni atom is negligibly small, although some properties such as the Curie temperature and crystallization temperature are strongly affected by the nickel replacement in amorphous Fe-Ni-B alloys.

On the basis of the previous experimental results [11], the first peak in $G(r)$ of Figs. 2 and 4 is interpreted as the superposition of the correlations of metal-metal and metal-metalloid pairs. But these correlations are not resolvable in the present results, because the contribution of metalloids (boron) to X-ray scattering intensity is small (about 6% of metal-metalloid pairs) in amorphous Fe-Ni-B alloys. The estimated numbers of near-neighbours in amorphous Fe-Ni-B alloys presently investigated are of the order of about 11.8 ± 0.3

(see Tables I and II). These values are slightly smaller than those ($n_1 \approx 13$) obtained in metallic glasses with phosphorus. This is consistent with the results of model calculation by the DRPHS model [19]. More information, however, is required such as the partial structures of the individual chemical constituents for quantitative discussion regarding the difference in the near-neighbour numbers between metallic glasses with boron and those with phosphorus.

Acknowledgements

The amorphous ribbons were made by W. R. Rollins. The authors express their thanks to C. M. Hanham for her technical assistance. The financial support from the National Science and Engineering Council of Canada is also greatly acknowledged.

References

1. J. L. WALTER, *Mater. Sci. Eng.* **39** (1979) 95.
2. Y. WASEDA and T. MASUMOTO, *Z. Physik* **B21** (1975) 235.
3. Y. WASEDA and H. S. CHEN, *Phys. Stat. Sol. (a)* **49** (1978) 387.
4. K. FURUKAWA, *Rep. Prog. Phys.* **25** (1962) 392.
5. P. ASCARELLI, *Phys. Rev.* **143** (1966) 36.
6. A. RAHMAN, *J. Chem. Phys.* **42** (1965) 3540.
7. Y. WASEDA and S. TAMAKI, *Phil. Mag.* **32** (1975) 273.
8. A. J. GREENFIELD, J. WELLENDORF and N. WISER, *Phys. Rev.* **A4** (1971) 1607.
9. R. KAPLOW, S. L. STRONG and B. L. AVERBACH, *ibid* **138** (1965) A1336.
10. A. H. NARTEN, D. M. DANFORDS and H. A. LEVY, *J. Chem. Phys.* **46** (1967) 4875.
11. Y. WASEDA, H. OKAZAKI and T. MASUMOTO, *J. Mater. Sci.* **12** (1977) 1927.
12. Y. WASEDA and H. S. CHEN, *Solid State Commun.* **27** (1978) 809.
13. C. H. BENNETT, *J. Appl. Phys.* **43** (1972) 272.
14. L. VON HEIMENDAHL, *J. Phys. F.* **5** (1975) L141.
15. R. YAMAMOTO, H. MATSUOKA and M. DOYAMA, *ibid* **7** (1977) L243.
16. T. EGAMI, R. S. WILLIAMS and Y. WASEDA, Proceedings of the 3rd International Conference on Rapidly Quenched Metals, Brighton 1978 (Metals Society, London, 1978) No. 198, p. 318.
17. E. NOLD, S. STEEB and P. LAMPARTER, *J. Appl. Phys.* in press.
18. D. S. BOUDREAX, "Amorphous Magnetism II", edited by R. A. Levy and R. Hasegawa (Plenum Press, New York, 1977) p. 463.
19. *Idem*, Abstracts of AIP Topical Symposium on the Atomic Scale Structure of Amorphous Solids, Yorktown Heights, New York, April (1978) p. L-8.
20. R. YAMAMOTO, T. MIHIRA, K. TAIRA and M. DOYAMA, *Phys. Letters* **70A** (1979) 41.

21. J. L. WALTER, S. F. BARTRAM and I. MELLA, *Mater. Sci. Eng.* **36** (1978) 193.
22. D. TURNBULL, *Scripta Met.* **11** (1977) 1131.
23. H. S. CHEN, J. T. KRAUSE and E. A. SIGETY, *J. Non-Crystalline Solids* **13** (1973/74) 321.
24. W. B. PEARSON, "Handbook of Lattice Spacing and Structure of Metals", Vol. 2. (Pergamon Press, Oxford, 1967).
25. L. BORNSTEIN, "Zahlenwerte und Funktionen aux Physik, Chemie, Astronomie, Geophysik und Technik", Band 1, Teil 4 (Springer-Verlag, Heidelberg, 1955).
26. D. E. POLK, *Scripta Met.* **4** (1970) 117; *Acta Met.* **20** (1972) 485.

Received 13 September and accepted 9 October 1979.